Instrumental Measurement of Bread Crumb Grain by Digital Image Analysis[1,2]

H. D. SAPIRSTEIN,[3] R. ROLLER,[3] and W. BUSHUK[3]

ABSTRACT

An instrumental system has been developed for direct quantitative assessment of bread crumb grain using digital image analysis technology implemented on a personal computer. Software was developed for comprehensive measurement of crumb grain features including cell area, cell density (cells/cm^2), cell-wall thickness, cell-total area ratio, crumb brightness, and uniformity of cell size. The system is completely objective in all respects, including the critical step of crumb cell detection, where an adaptation of the *K*-means algorithm was used for image segmentation by thresholding. Typical spatial resolution of the system using a conventional macroviewing lens was approximately (80 μm)^2 crumb per pixel. Image processing time to compute the crumb cell structure for a single bread slice (307,200 pixels per image) was about 10 sec. The precision and accuracy of the system were tested by analysis of results of experimental breadmaking using control and oxidant-formula loaves. Compared with control loaves, bread crumb containing oxidants was determined to be 6% brighter and to have, on average, 21% more cells/cm^2, 17% smaller cells in cross-sectional area, 13% thinner cell walls, and 16% more uniform grain. These values were consistent with the finer crumb grain of bread containing oxidants, as observed visually. The proportion of crumb comprising gas cells for control and oxidant-formula bread was precisely identical (46%). The equivalence provides objective evidence that the predominant difference in the crumb structure of bread prepared with and without oxidants relates almost exclusively to the degree of subdivision or coalescence of gas cells.

Cereal Chem. 71(4):383-391

Crumb grain has been defined as the exposed cell structure of crumb when a loaf of bread is sliced (Kamman 1970). As with bread scoring in general, the traditional basis for evaluation of crumb grain has been subjective, qualitative, and imprecise by nature. These limitations in characterizing the cell structure in baked bread have been recognized by cereal chemists for quite some time (Mohs 1924) and may explain why only limited information on bread scoring has been reported in the literature. Kilborn and Tipples (1981a) outlined an approach for visual evaluation of loaves in terms of cell-wall thickness, cell size, and crumb color; each was evaluated on a 10-point scale. A similar procedure was described by Swallow and Baruch (1986) for subjective assessment of a loaf's internal features in which cell size, uniformity of cell size, and thickness of cell walls were the main considerations. These features, in addition to cell shape, are generally considered to be important features reflecting flour strength, dough formulation, and processing. They help to define the quality of a loaf of bread to the baker and the consumer.

Given the technological relevance of crumb grain attributes (especially in the commercial production of white pan bread) and the limitations in evaluating quantitative bread crumb features in a qualitative fashion, the need for an instrumental method for objective measurement of crumb grain features seems clear. Digital image analysis, which has seen increasing use in the past decade for grain and grain product inspection and classification applications (Sapirstein 1993), offers a potential solution. A few studies using this technology in applications related to baking have been reported. Heyne et al (1985) used image analysis to quantitate the degree of brownness on the bottom surface of simulated pizza crusts to predict available lysine content in a nondestructive fashion. Smolarz et al (1989) showed that it was possible to describe the structure of extruded biscuits in terms of a few computed features, including biscuit cross-sectional area, detected cell area, cell orientation, and biscuit porosity. Bertrand et al (1992) derived mathematical descriptors related to visual grain features of bread crumb to evaluate the discrimination ability among french breads prepared with different emulsifiers. Zayas (1993) extracted pattern texture features from digital images of bread slices to differentiate bread from two commercial brands.

The goal of this research was to develop a working system on a personal computer (PC) for direct quantitation of technologically relevant crumb grain features. A necessary prerequisite was the implementation of an objective segmentation technique to classify monochrome images of bread slices into cells and background. An optimized straight-dough experimental breadmaking procedure was employed to evaluate the reproducibility of crumb grain measurements. Quantitation accuracy was evaluated by manipulating loaf volume and crumb grain by varying the level of oxidant in the formula.

MATERIALS AND METHODS

Flour and Baking

The flour used was milled from No. 1 Canada western red spring wheat of the 1989 crop year. It was of straight grade and contained 14.4% protein (N × 5.7) and 0.52% ash (both on 14%

[1]Presented at the AACC 77th Annual Meeting, Minneapolis, MN, September, 1992.
[2]Publication 215 of Department of Food Science, University of Manitoba, Winnipeg.
[3]Department of Food Science, University of Manitoba, Winnipeg.

mb). Bread (100-g flour basis) was prepared using the GRL-Chorleywood procedure as described (Kilborn and Tipples 1981b) without (control) and with 30 ppm (flour basis) potassium bromate and 37.5 ppm of ascorbic acid. Single loaves of control and oxidant-formula bread were baked on three successive days. After loaves were allowed to cool for 25 min, loaf volumes were measured and the bread was sliced transversely using an electric bread slicer to obtain slices of 12 mm thickness. Five central slices of each loaf were analyzed for crumb grain measurements; a single rectangular field of view (FOV) was evaluated for each slice (e.g., Fig. 1). A total of 30 digital images were processed and analyzed. This number was judged to be sufficient to evaluate the effectiveness and robustness of the crumb grain measurement system using experimental bread produced under controlled laboratory conditions.

Image Analysis System

All measurements used a customized PC image analysis system described previously (Sapirstein et al 1987), but it was considerably modified for this study. Digitization and preprocessing of RS-170 video camera output used a PC-Vision Plus (square-pixel option) image frame grabber (Imaging Technology, Inc., Bedford, MA). The frame grabber was implemented in a 486-AT PC that provided 256 gray level (GL) digital images, each comprising 640 columns by 480 rows of picture elements (pixels). The camera used was a monochrome charge-coupled device (Panasonic WV-CD50), fitted with a 50-mm *f*-1.4 fixed-focus C-mount lens (Fujinon Inc.) using 12 mm of extension. Camera gain and offset values were 50 and 58, respectively. These settings were empirically determined to provide images of suitable contrast within the GL response range of the digitizer (e.g., Fig. 2), to optimize the dynamic range of GL values for digital images of bread slices. Software for the crumb grain measurement system, developed in our laboratory, was written in the C language (Microsoft C 5.1) and was used on the system's 486 DX/33 PC running the DOS 5.0 operating system.

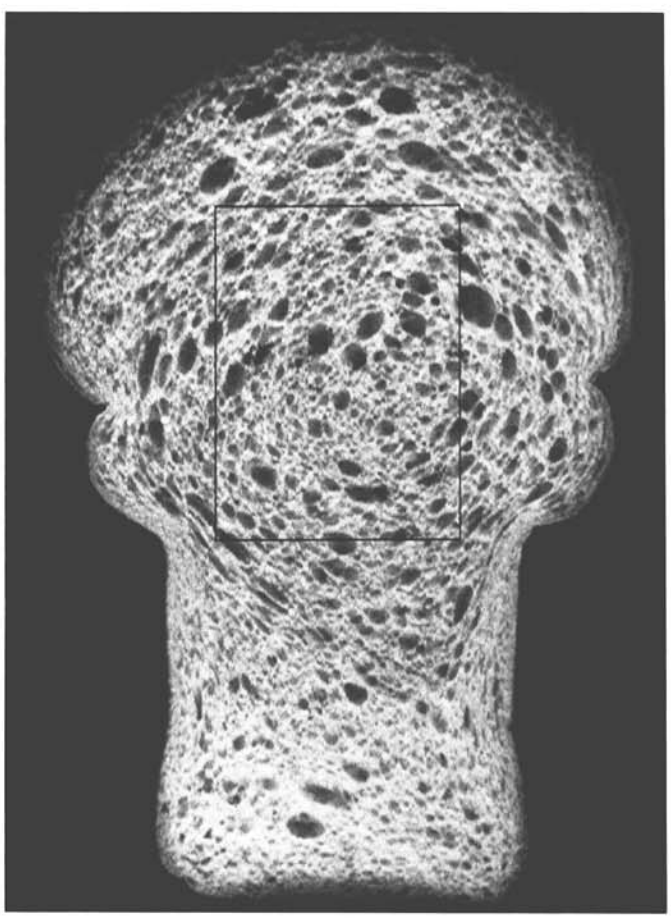

Fig. 1. Gray level image of a slice of bread illustrating the typical size and position of crumb areas that were analyzed.

Viewing of Bread Slices and Image Calibration

Bread slices were examined from a distance (lens to object) of 28.2 cm in reflected light using a conventional 90° detection, 45° illumination configuration. The FOV was 46 × 35 mm, which represented approximately one-quarter to one-third of the cross-sectional area of experimental bread slices. Figure 1 illustrates a digital image of a bread slice showing the typical size and position of the area surveyed, which was located in the top half of the slices. Spatial resolution was approximately (80 μm)^2 crumb per pixel. Metric measurements of crumb grain were obtained by normalizing pixel data using the diameter of a Canadian 10-cent coin (diameter: 18.034 mm) computed from digital images.

Lighting was provided by four incandescent tungsten-filament frosted envelope lamps (Spectro 40 W; color temperature 2,750° K) in a ring configuration. The working standard for normalization of the imaging system's GL (reflectance) response was a small section of white opal acrylic plastic, 2 mm thick. Reflectance normalization was empirical and was performed before each image acquisition session. A central area of interest on the reflectance standard was repeatedly digitized, and the lens aperture was manually adjusted until the computed mean GL corresponded to a predetermined target GL value (160), which corresponded to 79% reflectance. This value was close to the mean reflectance of the analyzed bread crumb. The precision of reflectance determination was routinely better than 1%.

GL was calibrated to reflectance using a 12-step calibrated paper gray scale (cat. 152 2267, Kodak, Rochester, NY). Although the 8-bit digitizer of the frame grabber could quantitate 256 GL steps, the actual contrast or dynamic range of GL response was ~170–180 arbitrary units (Fig. 2). This corresponded to ~65% on a calibrated reflectance scale (from 35% to just under 100% reflectance). This was more than sufficient for purposes of quantitation.

Image Segmentation

The segmentation of a digitized image describes a process that extracts coherent information from raw image data. It is the critical first step that links image acquisition with pattern recognition and analysis. Thresholding is a popular image segmentation tool that reduces the complexity of digital image data varying on a continuous scale by reducing the number of GLs, for example, to two levels by global thresholding where an entire image is partitioned by a single threshold value to create a binary image. For images of white pan bread, an optimal binary image can be generated by selecting a single appropriate GL threshold; pixels with GL values lower than those of the threshold would be deemed to be constituents of cells. What is a correct threshold, and how to find it, are the key questions.

An appropriate GL threshold may be found interactively (subjectively) by varying the GL until the binary image conserves the essential features of the monochrome counterpart. This was the approach used by Smolarz et al (1989) for image analysis of extruded biscuits. Experimentation with this procedure showed it to be unreliable, as even small deviations in the GL threshold resulted in substantial variations in computed crumb grain features.

Numerous objective thresholding methods for image segmentation are described in the literature (Haralick and Shapiro 1985, Sahoo et al 1988). In the simplest of cases, an optimal threshold may be easily determined from the GL histogram, assuming that the image is of the right kind (composed of uniformly bright or dark objects on a contrasting background). These conditions typically result in a bimodal histogram. Unfortunately, GL histograms of bread crumb were unimodal (Fig. 2).

In the present study, the aim was to objectively determine a threshold for accurate perception of crumb cells and subsequent quantitation of crumb grain features. This objective was met by using an image segmentation approach based on adapting a cluster

analysis method commonly known as the *K*-means algorithm (Hartigan 1975). For each bread slice examined, an optimum GL threshold to divide images into regions of cells and background was obtained.

In general, the algorithm groups a set of data that contains *M* observations described by *N* variables or features into *K* clusters, each with its own unique characteristics. For the crumb grain measurement problem, the computation was simplified in two aspects. First, the number of variables was reduced to one, as pixel GL was the only attribute under consideration. Second, the number of possible clusters was limited, owing to the physical nature of a bread slice. At the cut surface of a bread slice, the random three-dimensional spongelike arrangement of gas cells embedded in a glutinous starch matrix is revealed as a two-dimensional pattern of dark cells on a bright background. Each image is apparently a two-cluster problem, although cells may be graded or classified based on reflectance, which would increase the number of clusters by a limited amount. The presence of dark-colored ingredients in a bread formulation, such as poppy seeds, raisins, etc., would also tend to increase the number of natural clusters that are feasible. In general, the usefulness of information beyond three or four clusters is probably limited, particularly in the case of a basic white bread formula. This article presents results for two- and three-cluster *K*-means analysis. The algorithm was computationally efficient; the time to compute the critical GL threshold for two- or three-cluster partitions was ~2–3 sec per image.

Step 1. Group the GL histogram *H[I]* into a partition *P(M,K)* with *K* clusters of *M* GL values, each divided by *K*−*1* boundaries. Where $K = 2$, the search for the boundary or partition point begins by using the median GL value of *H[I]*. For $K > 2$, the initial values for cluster boundaries were assigned at GL values that were evenly distributed across *H[I]*. After the initial boundary allocation, a measure of grouping efficiency was determined. This is denoted by the partition error (PE = e[*P(M,K)*]), which can be defined as:

$$\mathrm{PE} = \mathrm{e}[P(M,K)] = \Sigma_{I=1}^{M}\, D[I,L(I)]^2$$

where *M* is the number of GL elements (e.g., 256) in *H[I]*, and *L(I)* is the cluster in which the GL value *I* is a member. *D(I,L)* is the euclidean distance between the *I*th GL value in the partition and the mean GL value, *B(L)*, of all the elements in the *L*th cluster, and is defined as:

$$D(I,L) = \sqrt{[I - B(L)]^2}$$

and by elimination of the squared factor to increase computational efficiency, it can be simplified to:

$$D(I) = |[A(I) - B(L)]|$$

The value of the histogram stored in *H[I]* provides a weight factor for all distance calculations, and it is equivalent to the number of pixels in the set of points with GL values of *I*. The above definitions can now be restated as:

$$\mathrm{e}[P(M,K)] = \Sigma_{I=1}^{M}\, (H[I] \times D[I])$$

which is the implementation of the PE.

Step 2. Move the lowest cluster boundary, and shift the partition down, to move an object that is on the edge of the lower cluster into the higher one. With the object moved, the PE is once again calculated and compared with the previous calculation. If PE is reduced, the process is again repeated until it no longer decreases. Once the minimum is found, the location of the partition boundary is stored along with the value of the PE.

The above procedure is repeated based on upward shifting of

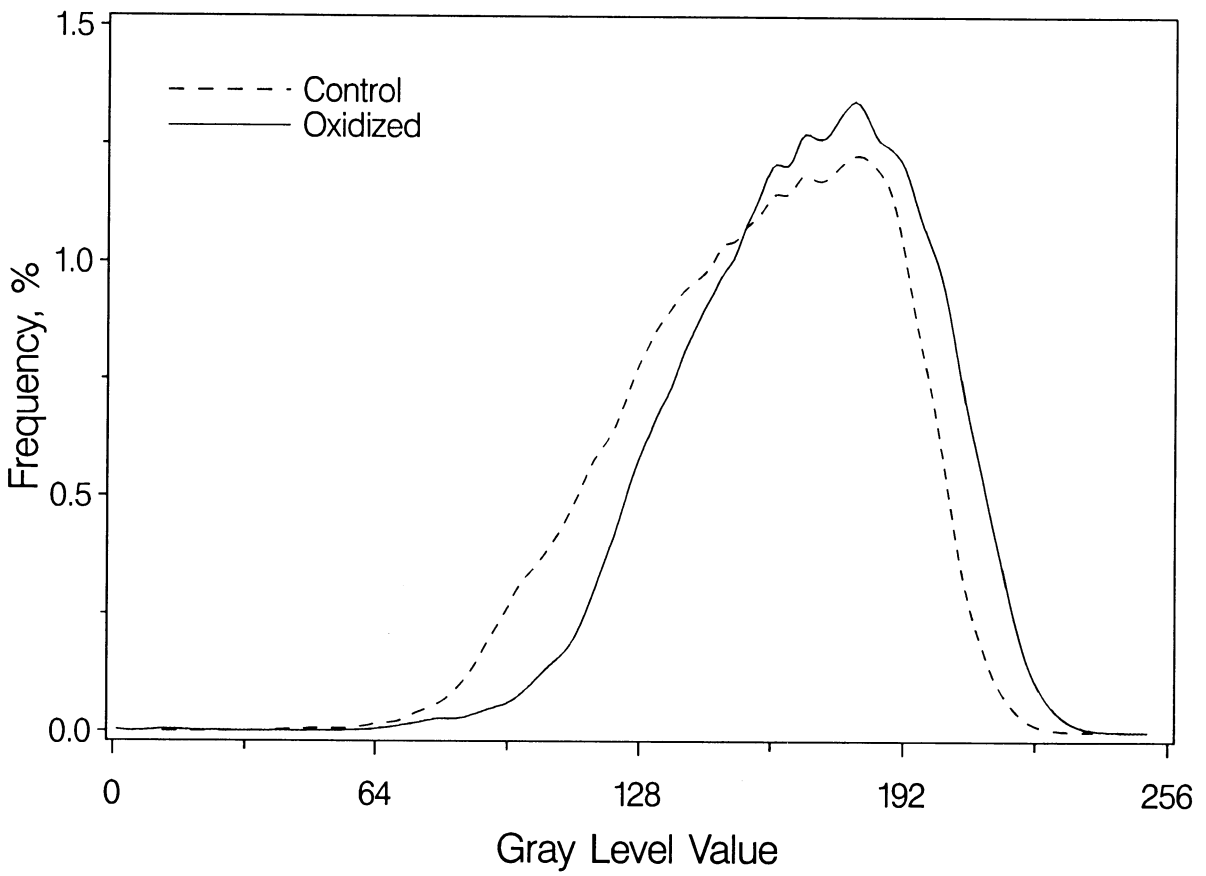

Fig. 2. Gray level histograms of digital images of bread crumb from single loaves of control and oxidant-formula bread prepared on Day 2. Brightness increases from left to right. Each histogram represents the mean of bread crumb images derived from five slices.

the partition boundary. With each shift, PE is determined and compared with the previously calculated value. Once a minimum is found, the two minima are compared, and the lowest one is used as the new PE.

Step 3. Repeat Step 2 for all other partitions (3, 4, . . ., K), and make any changes to the partition boundary locations as needed to reduce the PE.

Step 4. Check whether any changes occurred to the partition boundaries in Steps 2 and 3. If there were no changes, the processing is complete. If any change did occur, Steps 2 and 3 are repeated until no changes occur, using the lowest PE found initially for comparison.

Completing the above procedure provides the optimum clustering of the histogram into K clusters. Regardless of the number of partition boundaries, the boundary point (determined by Step 4) with the lowest value was subsequently used as the GL threshold value for image binarization and cell detection.

Cell Detection and Computation of Crumb Grain Features

Cell detection in binary images was based on an algorithm that considers cells to be any connected region of pixels with GL values lower than a specified threshold. In the present study, isolated single pixels were considered to be valid cells as long as they satisfied the thresholding criterion. Isolated single pixels, ~80 μm in diameter, constituted the most frequent class of detected cells.

For comparison of control and oxidant-formula bread, computation of crumb grain features was based on two different threshold specifications. First, the K-means algorithm threshold was determined for control slices. The mean threshold value for individual loaves was applied for crumb grain measurement of both control and oxidant-formula bread. This was referred to as cell detection and crumb grain measurement by fixed GL thresholding. Second, the analysis of oxidant-formula bread was based on a K-means algorithm threshold specific for this type of bread. This procedure was referred to as optimized GL thresholding. The fixed GL thresholding approach yielded erroneous data for oxidant-formula bread (as discussed below).

Although the GL threshold had a significant impact on the derived crumb grain feature values, algorithms to derive the features were GL-independent. Six quantitative features of bread crumb were computed: 1) number of cells, 2) number of cells/cm^2, 3) mean cell area, 4) cell-total area ratio, 5) cell-wall thickness, and 6) crumb brightness, expressed as the mean FOV GL. Additionally, for each bread slice analyzed, the frequency distribution of cell sizes was evaluated to obtain a derived parameter related to crumb grain uniformity.

The number of cells/cm^2 represents the density of cells independent of the magnitude of cross-sectional area of the FOV; larger values denote finer crumb structure.

Cell-total area ratio corresponds to the proportion of the crumb area computed as cells. For N detected cells, this parameter was computed as:

$$\text{Cell-total area ratio} = (\Sigma_{I=1}^{N} \text{cell area})/\text{total area surveyed}$$

Cell-total area ratio represents a measure of system performance to detect cells, as well as being a basic parameter of the cell structure of the crumb.

Cell-wall thickness (CWT) was calculated as the average value of a distance measure, repeated for all detected cells, between the boundaries of a given cell and the boundaries of cells detected at regular angular intervals in its neighborhood. Starting with the first cell in a list of detected cells, the centroid (X_c, Y_c) of the cell was determined by summing the coordinates of all pixels within the area of the cell:

$$X_c = (\Sigma_{i=1}^{P} X_i)/P$$

$$Y_c = (\Sigma_{i=1}^{P} Y_i)/P$$

where P is the number of pixels in the cell; X_i is the X coordinate of the pixel in the cell; and Y_i is the Y coordinate of the pixel in the cell.

A check was then made to determine whether the calculated centroid existed within the detected region of the cell. Infrequently, a cell with irregular shape generated a centroid lying outside the cell boundary. This occurred with a frequency of ~5%. CWT values were not computed for these cells, which were used only as neighboring objects in the calculation.

Distance measures between a given cell and its neighbors were determined using an algorithm employing vectors originating at the cell centroid and dispersed at fixed-angle increments Δ(e.g., 15°). The angle θ ($0 \leq \theta \leq 360$) was defined as: $\theta = n\Delta$, where n was a positive integer ($n \geq 0$) defining the number of measurements performed for each cell.

A search was performed for two boundary points by moving along a selected vector. The first was the boundary of the starting, or current, cell (X_0, Y_0); the second was the boundary (X_1, Y_1) of the first neighboring cell detected along the vector. To minimize erroneous data, two checks were performed in this cell-boundary search. The first was made to evaluate whether the edge of the image frame was reached before a boundary was encountered. If this occurred, CWT for the current cell along this vector was set to 0. The second check was to evaluate whether the detected border at (X_1, Y_1) was part of the current cell. If true, the current cell boundary (X_0, Y_0) was replaced with the coordinates (X_1, Y_1), and the search is continued along the vector for the boundary of a neighboring cell. Once the two boundary coordinates are found, the CWT was calculated as:

$$\text{CWT} = \sqrt{(X_1 - X_0)^2 + (Y_1 - Y_0)^2}$$

The above process was repeated for all detected cells. An average CWT was calculated based on individual CWT with values >0. A Δ value of ≤30° (≥12 vectors/cell) was determined to be a satisfactory increment. Results based on $\Delta = 15°$ (24 vectors/cell) are reported in this article.

RESULTS AND DISCUSSION

Baking Results

Baking results (Table I) showed very little difference in final proof height between control and oxidized doughs using a constant proof time of 55 min. If a difference in gas retention capacity of the fermenting doughs actually existed, this difference was only marginally expressed with the relatively short proof times used. The expected improver effect related to oxidation was clearly manifested during baking; there was, on average, an increase of ~30% in the loaf volume of bread prepared with oxidants. There appeared to be a trend for loaf volumes to decline slightly for bread prepared on successive days. As expected, bread prepared with oxidants had noticeably finer crumb grain.

TABLE I
Baking Results

	Final Proof Height (mm)		Loaf Volume (cm^3)	
	Control	Oxidized	Control	Oxidized
Day 1	104	106	740	970
Day 2	104	107	735	950
Day 3	105	107	725	940
Average	104 ± 1	107 ± 1	733 ± 8	953 ± 15

Image Histograms and Segmentation

The GL histograms of digital images of white pan bread (Fig. 2) were characteristically unimodal in shape, indicating that reflectance of bread crumb was expressed in a continuous fashion. Figure 2 shows that the histograms were slightly skewed towards lower GL values. Corresponding histograms for control and oxidant-formula bread baked on different days were virtually identical to those shown in Figure 2. There was little or no

difference in the peak GL for respective slices of control and oxidant-formula bread; the maxima occured predominantly at GL 166 (81% reflectance). Compared to control loaves, image histograms of oxidant-formula bread possessed a significantly higher frequency of pixels at the maximum, and they were invariably shifted to the right, indicative of bread with a marginally brighter crumb appearance.

Examining bread slices visually gives a basic perception of crumb grain structure composed of distinctively dark cells on a contrasting white background. It might therefore be expected that corresponding images would yield bimodal histograms. This would make image segmentation a relatively straightforward process of finding the valley point between the two modes to establish the critical GL threshold to localize cells via image binarization, a commonly used procedure (Prewitt and Mendelsohn 1966, Haralick and Shapiro 1985). However, the unimodal nature of the image histograms (Fig. 2) indicates that crumb cells had a broad range of GL values with a sufficiently high frequency of relatively bright (mid-range GL) pixels that would obscure cell distinctiveness in image histograms. This outcome is likely derived from the predominance of detected small cells that characteristically possess relatively high reflectance.

Despite the complex nature of crumb grain and the seemingly unremarkable appearance of crumb grain image histograms, implementation of the *K*-means cluster analysis algorithm yielded extremely consistent and apparently accurate segmentation results. Figure 3 shows a typical result of image segmentation using this approach for slices from control and oxidized loaves. Binarization using GL threshold derived by the two-cluster *K*-means algorithm (Fig. 3B and E) essentially preserves the total crumb grain structure of the corresponding GL images (Fig. 3A and D) for the control and oxidized bread slices, respectively. Compared with the GL images, the binarization process also appears to clarify the essential features of these images. The two-cluster segmentation results clearly show that the oxidized bread slice (Fig. 3E) is filled with a greater number of smaller cells. Also, cells in the oxidized slice appear to be more elongated when compared with those in the slice from the control bread. The contributory effects of dough molding and subsequent proofing, particularly in the presence of oxidants, to the cell structure of bread has been reported (Baker and Mize 1941). Elongated cell shape probably arose from the sheeting and stretching action of the molder used (Kilborn and Irvine 1963). It was a typical characteristic of the oxidant-formula bread. Although cell shape was not measured in this study, such an investigation seems to be warranted because elongated cell shape is generally regarded as a positive attribute in bread scoring (Kamman 1970, Pyler 1988).

The corresponding binary images using the GL threshold generated by the three-cluster *K*-means algorithm (Fig. 3C and F) preserve the cell composition of the GL images for cells, or portions thereof, which are darker in appearance. Compared with the two-cluster segmentation result, the proportion of the FOV comprising cells from the three-cluster result was lower. Close inspection of the two- and three-cluster binary images reveals that in the latter there was considerable erosion of the periphery of many of the cells. In some cases, interconnected cells in the two-cluster binarization have separated due to the erosion effect as a consequence of using a lower GL threshold for image segmentation. The number of detected cells per image was not affected as much as the cell areas.

Crumb Grain Feature Values and Data Reproducibility

Typical crumb grain measurement results for five consecutive slices of a control loaf are presented in Table II. These data were generated with crumb cell detection for all slices based on the same *K*-means GL threshold (155). This value corresponded to the mean computed for the five slices. The two-cluster computed GL threshold among slices of an individual loaf never deviated from the mean by more than two GL units. Accordingly, calculation of crumb grain features on the basis of digital images segmented using an average GL threshold for each loaf, or based on a threshold value computed for each slice, gave similar results. As the latter approach is more efficient and resulted in slightly better data precision over all features, it probably represents the preferred method for routine analysis.

The data in Table II are representative of the typical values of computed crumb grain features determined for control formula bread. Given the high cell count densities of 93–100 cells/cm^2, mean cell areas were correspondingly small. Averaged over all

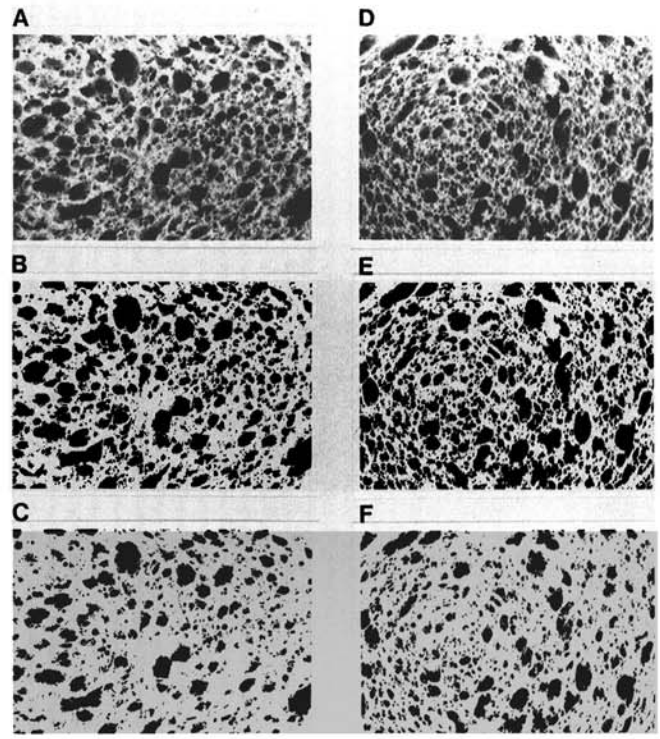

Fig. 3. Digital images of control (left) and oxidant-formula bread (right), showing the original gray level images (**A** and **D**), along with the computed binary results from gray level thresholding at the two-cluster (**B** and **E**) and three-cluster (**C** and **F**) *K*-means algorithm determined values. Corresponding histograms for panels **A** and **D** are presented in Figure 2.

TABLE II
Typical Computed Bread Crumb Grain Features for Consecutive Slices of an Individual Pup Loaf[a]

Slice	Number of Cells Detected	Cell Density (cells/cm^2)	Mean Cell Area (mm^2)	Cell-Total Area Ratio	Cell-Wall Thickness (mm)	Field of View Gray Level[b]
1	1,578	98	0.474	0.463	0.851	156
2	1,613	100	0.443	0.442	0.914	157
3	1,527	94	0.476	0.449	0.909	155
4	1,498	93	0.481	0.446	0.930	157
5	1,605	99	0.454	0.451	0.912	156

[a] Control dough formula (no oxidants); gray level threshold for image binarization (155) was the average *K*-means threshold for the five slices.
[b] A measure of crumb brightness.

the slices, a mean cell area of 0.47 mm^2 corresponded to a cell equivalent diameter of:

$$2\sqrt{\text{area}/\pi}$$

based on circular cell shape of ~700 μm. This appears to be a reasonable value from visual inspection of the bread slices. Cell-total area ratios were 0.44–0.46. Thus, based on the FOV analyzed, ~45% of the bread cross-sectional area comprised gas cells. This interesting figure also seems plausible based on experience. CWT for the control formula bread slices was 0.85–0.93 mm. This most probably represents an overestimation of actual CWT in uncut bread. The overestimation derives from the likelihood that only a small proportion of neighboring crumb cells exposed on the cut surface of a slice of bread are actually bisected, which is a prerequisite for generating a minimum CWT value. Nevertheless, the CWT computation accurately reflects the analysis result for the typically large population of detected cells (>1,500) in digital images of bread slice sections.

The crumb grain feature measurements (Table II) for consecutive slices of an individual control formula loaf are typical of the level of variation in the data as a whole. Slice-to-slice variation for the control, expressed as the coefficient of variation (CV) averaged over three days for number of detected cells, cell density, cell area, cell-total area ratio, CWT, and FOV GL was 6.1, 5.8, 7.6, 3.1, 4.1, and 0.4%, respectively. There was no significant difference in slice-to-slice CV of computed features between control and oxidized-formula bread. While the variability in crumb grain features among slices of individual loaves was relatively low, the data indicate the need for some limited sampling (at least two slices) to ensure that representative data are obtained for each loaf. Crumb brightness calculated as the image mean GL was the most reproducible of the features that were measured.

Compared with slice-to-slice variability, data for loaves baked on different days (Table III) was comparatively more precise, with the exception of the CWT calculations. Analysis of variance and Duncan's multiple range test results indicated there were no significant differences ($P < 0.05$) for any of the grain features for bread baked on different days, with the exception of CWT. Control loaves baked on Days 2 and 3 yielded bread with significantly ($P < 0.05$) thinner cell walls than those baked on Day 1. CWT for control loaves showed a declining trend for bread baked on consecutive days. This trend appears to be related to corresponding loaf volumes (Table I), which became marginally lower with each successive day. Whether this pattern in the data occurred by chance or as a result of some factor related to dough formulation (e.g., yeast activity or processing) is not known. No similar relationship was observed for oxidant-formula bread. In contrast, oxidized loaves baked on Day 3 were distinguished by having significantly thicker cell walls, on average, than did bread baked on preceding days. This phenomenon was not studied further.

Comparison of Crumb Grain Measurements for Control and Oxidant-Formula Breads

In line with loaf volume results (Table I), substantial differences were found in the computed bread crumb features for loaves baked with and without oxidants (Table IV). Additionally, the magnitude or direction of difference for some features varied with the computational procedure, depending upon the use of fixed or optimized GL thresholding for image segmentation. These data are summarized in Table V.

TABLE III
Reproducibility of Computed Crumb Grain Features for Control and Oxidant-Formula Bread Baked on Different Days[a]

	Number of Cells Detected	Cell Density (cells/cm^2)	Mean Cell Area (mm^2)	Cell-Total Area Ratio	Cell-Wall Thickness (mm)	Field of View Gray Level[b]
Control						
Day 1	1,567 ± 51	97 ± 3	0.47 ± .02	0.45 ± .008	0.90 ± .03	156.2 ± 0.8
Day 2	1,590 ± 170	98 ± 10	0.47 ± .06	0.45 ± .02	0.87 ± .05	156.6 ± 1.9
Day 3	1,570 ± 70	97 ± 4	0.49 ± .02	0.47 ± .001	0.81 ± .03	155.0 ± 0
Mean	1,571 ± 5	97 ± 0.6	0.48 ± .01	0.46 ± 0.01	0.85 ± .05	155.9 ± 0.8
CV, %[c]	0.3	0.6	2.3	2.2	5.6	0.5
Oxidized						
Day 1	1,871 ± 124	116 ± 8	0.40 ± .03	0.46 ± .004	0.73 ± .02	165.4 ± 0.5
Day 2	1,942 ± 141	121 ± 9	0.39 ± .04	0.46 ± .01	0.72 ± .04	164.8 ± 1.1
Day 3	1,834 ± 122	114 ± 8	0.40 ± .04	0.45 ± .02	0.83 ± .04	163.0 ± 1.4
Mean	1,882 ± 55	117 ± 3	0.40 ± .01	0.46 ± .006	0.76 ± .06	164.4 ± 1.2
CV, %	2.9	3.4	2.6	1.3	8.1	0.8

[a] Gray level threshold for image binarization was the average *K*-means gray level threshold for each loaf. For control and oxidant-formula bread, the mean threshold values were 155 ± 1 and 164 ± 2, respectively.
[b] A measure of crumb brightness.
[c] Coefficient of variation.

TABLE IV
Effect of Computing Procedure on Crumb Grain Features of Bread Prepared With and Without Oxidants

Cell Detection Method	Gray Level (GL) Threshold for Cell Detection	Cell Density (cells/cm^2)	Mean Cell Area (mm^2)	Cell-Total Area Ratio	Cell-Wall Thickness (mm)
1[a]					
Control	155	98 ± 1	0.47 ± .01	0.46 ± .01	0.86 ± .05
Oxidized	155	128 ± 9	0.28 ± .03	0.35 ± .02	1.03 ± .04
2[b]					
Control	155 ± 1	97 ± 1	0.48 ± .01	0.46 ± .01	0.85 ± .05
Oxidized	164 ± 2	117 ± 3	0.40 ± .01	0.46 ± .01	0.74 ± .03
3[c]					
Control	137 ± 0	95 ± 6	0.30 ± .01	0.27 ± .01	1.57 ± .10
Oxidized	146 ± 3	126 ± 6	0.22 ± .01	0.27 ± .01	1.45 ± .21

[a] Fixed GL threshold (155) from control loaf analysis.
[b] Optimized GL thresholding (2 clusters) for control and oxidized loaves.
[c] Optimized GL thresholding (3 clusters) for control and oxidized loaves.

An obvious question arises as to which, if either, of the two computational procedures (fixed vs. optimized GL thresholding) generates the most accurate data. There is no reference method for crumb grain measurement to use as a benchmark. However, we do have certain expectations of how a bake test affects loaf volume and crumb grain, particularly when the only treatment variable is the level of oxidant in the formulation.

Compared to the optimized approach, the fixed GL thresholding resulted in a larger degree of difference in crumb grain measurements between control and oxidant-formula bread. Compared to control loaves, the oxidant-formula bread had, on average, 31% more cells/cm^2 that were 40% smaller in size. While this magnitude of difference appears plausible, the data for both cell-total area ratio and CWT appear to be incorrect. Given the finer crumb grain of the oxidized loaves, thinner cell walls would be expected; a 20% increase of CWT is therefore an erroneous result. Additionally, one could reasonably expect that the proportion of the crumb detected as cells in the oxidant-formula bread would at least be equivalent to that for the control, but the cell-total area ratio value was 24% lower.

Accordingly, while the fixed GL thresholding cell-detection method has the advantage of simplicity, it seems to generate some inaccurate data. The problem could be caused by the difference in crumb brightness between the control and the oxidant-formula bread. The relative difference in brightness was ~8 GL units (Table III), or 3% on a calibrated reflectance scale. Oxidized slices with smaller and more numerous gas cells, which is consistent with a finer cell structure, were marginally whiter in appearance. Therefore, applying a fixed GL threshold, based on unoxidized bread, yields a lower than optimum GL for cell detection of oxidized loaves. The result is an underestimation of the cell size that leads to erroneous results for other related parameters, such as CWT. Analogous results would be obtained if oxidant-formula bread were to be used as the basis for deriving a GL threshold for processing and analysis of all the digital images; unoxidized bread would have overestimated cell sizes and underestimated CWT (results not shown).

The effect of the GL thresholding procedure on the relative change in crumb grain features for oxidant-formula bread relative to that of the control (Table V) provides clear evidence for the magnitude of the errors that can be generated by shifting the GL threshold (for oxidant-formula bread) by only 8 GL units, or ~3% of full scale. In contrast, such a small shift in reflectance was barely noticeable by visual inspection of the binarized images

TABLE V
Effect of Computing Procedure on the Relative Change (%) in Crumb Grain Features on Addition of Oxidants

Crumb Cell Detection Method	Cell Density	Cell Area	Cell-Total Area Ratio	Cell-Wall Thickness
Fixed gray level (GL) thresholding	31	−40	−24	20
Optimized GL thresholding (2-cluster)	21	−17	0	−13
Optimized GL thresholding (3-cluster)	32	−24	0	−8

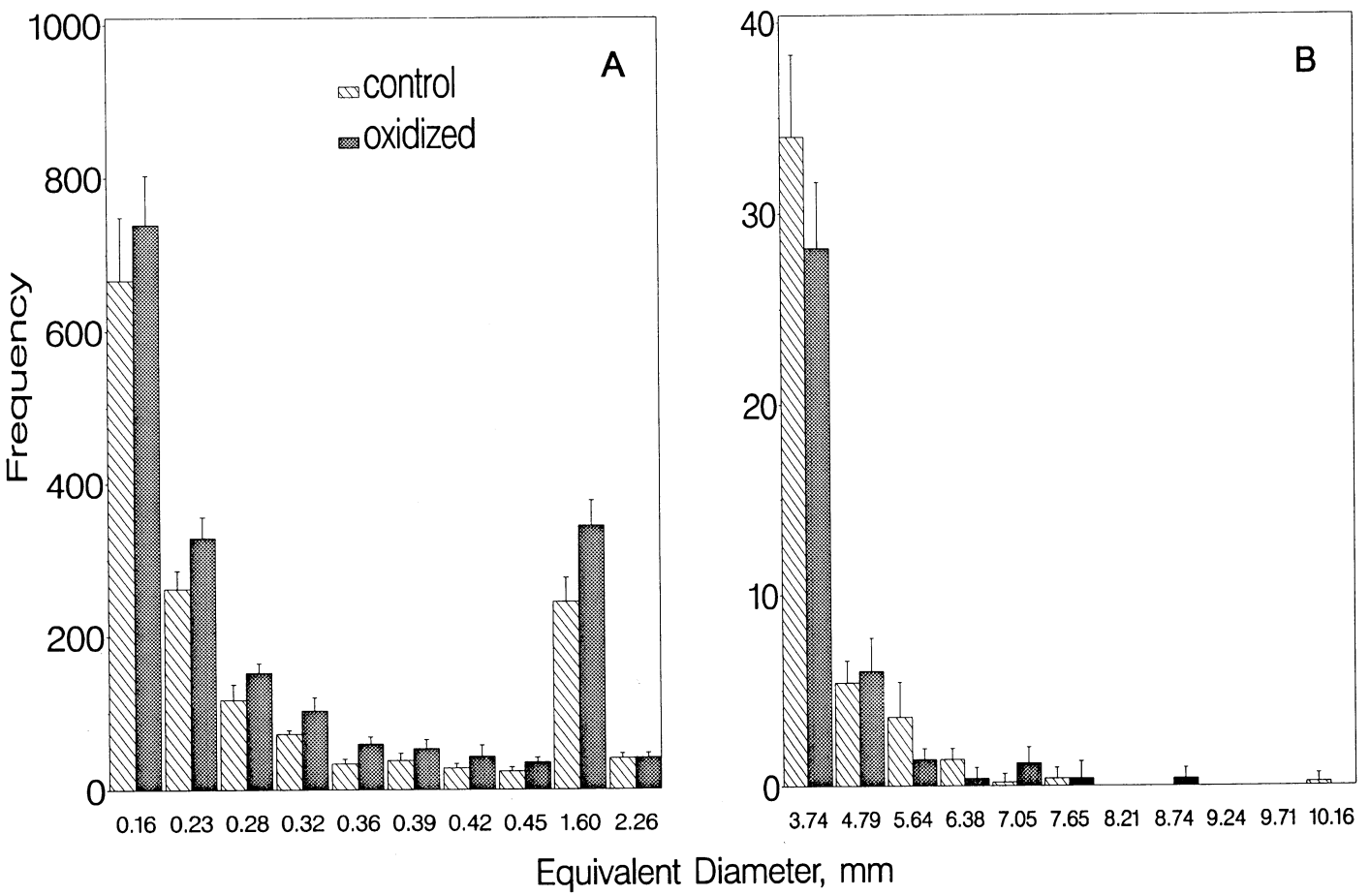

Fig. 4. Frequency distributions of small (**A**) and large (**B**) crumb cells for control and oxidant-formula bread computed by optimized two-cluster *K*-means gray level thresholding of digital images of Day 2 bread slices. Data corresponds to the mean of five slices; error bars represent one standard deviation. The two histograms for each equivalent diameter represent cell counts in the size range between the preceding (minimum) and indicated (maximum) value. The minimum equivalent diameter denoted by the first histogram pair was 0.080 mm.

or of the bread slices themselves. Accordingly, assignment of critical GL thresholds for image processing by subjective means should be avoided. It can be concluded that instrumental crumb grain measurement requires optimized cell detection, specific to the type of bread or breadmaking procedure, to account for differences in crumb brightness that may occur.

Optimized thresholding (two-cluster), whereby different GL threshold values were used to segment images for control and oxidized slices, resulted in 21% more cells that were 17% smaller in area with 13% thinner cell walls, These values are consistent with the appearance of the grain assessed visually. The cell-total area ratio results (0.46) are noteworthy, as optimized cell detection procedures give precisely equivalent values for the oxidized and control slices: 46% of the cross-sectional area (and consequently volume) of bread was determined to comprise gas cells. We believe the equivalence of these numbers to be accurate. These data indicate that the predominant difference in the crumb structure of bread prepared with and without oxidants relates exclusively to the degree of subdivision or coalescence of gas cells. A cell-total area ratio of 0.46 may be unique to the experimental short-time breadmaking process used in this study. It remains to be determined whether other breadmaking procedures have similar or distinct values.

Baker and Mize (1941) clearly demonstrated that the integrity of gas cells in weaker (unoxidized) dough compared with those in stronger (optimally oxidized) dough, cannot be maintained throughout the course of gluten development, proofing, and baking. As a consequence, small gas cells coalesce into larger ones. In the absence of other effects, the greater the degree of gas cell coalescence during the breadmaking process, the coarser the resulting bread crumb structure. Intuitively, the coalescence process should have no effect on the proportion of the volume or cross-sectional area of bread comprising gas cells. The equivalence of cell-total area ratio values for control and oxidized slices obtained in this study provide, for the first time, objective evidence in complete agreement with the classical subjective interpretation of the cell structure of bread.

Frequency Distribution of Crumb Cell Size and Crumb Grain Uniformity

A comparison of histograms for gas cell equivalent diameters for control and oxidant-formula bread is shown in Figure 4. Gas cells ranged in size from 80 μm to ~10 mm. The mean cell size for control and oxidant-formula bread, averaged over all loaves, was 774 and 714 μm, respectively. The majority of cells are much smaller in size than the average. This is consistent with the progressive increase in the frequency of crumb cells with decreasing cell size. This practical result derives from the theory of bubble mechanics and the relationship $p = 2y/r$ for a spherical bubble in equilibrium, where the internal pressure (p) of a gas cell is related directly to the surface tension (y) at the gas-liquid interface, and inversely related to the cell radius. Thus, in a system where the interfacial tension does not vary (as in a dough), there will be a tendency for leavening gas to seek larger gas cells (Handleman et al 1961). For dough, and ultimately for bread, the expected outcome would be a distribution of cell sizes substantially skewed towards smaller cells (Fig. 4). The spatial resolution limit of the imaging system did not permit detection and measurement of cells smaller than 80 μm equivalent diameter. However, the histogram result suggests that gas cells of this size were present in the greatest number. Determining what the limiting size of gas cells is in bread will require an imaging system of higher resolution than the one used in this study.

We attempted to localize the smallest gas cells in the digital images by using pseudocolor to enhance the visualization of cells corresponding to a maximum of one to five neighboring pixels (results not shown). The smallest gas cells visible in these digital images, which already represented a considerably magnified field (~25× in cross-sectional area), were ~160 μm in diameter and comprised two contiguous pixels. These cells were, for the most part, located in the walls surrounding larger cells. These may correspond to the intramural cells observed by Burhans and Clapp (1942), which were reported as numerous new bubbles appearing in the walls of preexisting ones during the oven-spring phase of baking.

To facilitate satisfactory graphic display of the distribution of computed bread crumb cell sizes, the histograms of Figure 4 were separated into two size classes. The separation point at an equivalent diameter of 2.26 mm corresponds to the mean cell area (~4 mm^2), below and above which, there is a distinct change in the relative frequency of cells found in control and oxidant-formula bread. In the cell sizes of 80–1,600 μm, the oxidant-formula bread had 15–40% more cells/cm^2 than did the control bread. The apparent discontinuity in the number of cells at 1,600 μm occurred because the size interval (1,150 μm) associated with this histogram point covered ~38× the range of the preceding interval size (30 μm). For the relatively larger cells (Fig. 4B), 2.2–10 mm equivalent diameter, this pattern of difference was reversed. Control loaves tended to have more cells in each cell size class, which is consistent with the coarser crumb grain of these loaves. However, the difference was surprisingly small; averaged over all loaves, the number of large cells in control and oxidant-formula bread was 44 ± 2 and 39 ± 3, respectively. In addition, control loaves did not always generate the largest cells, which ranged in size from ~8–10 mm equivalent diameter.

While the number of cells detected with equivalent diameters >2.26 mm represented a very small proportion (<3%) of the total number of detected cells (Table VI), they represented a substantial proportion of the total area. On average, large cells accounted for approximately 2.8 and 2.1% of total cell counts and 59 and 54% of total crumb cell area for control and oxidant-formula bread, respectively. While these differences appear small, statistically they were highly significant ($P < 0.01$). It is important to note that the proportion of large cells relative to total cell area for Day 3 oxidant-formula bread was significantly higher than that of the oxidant-formula bread prepared on other days (Table VI). Interestingly, there was no significant difference in the proportionate number of large cells for oxidant-formula bread baked on other days. We further quantified the influence of large cells by calculating the ratio of large-to-small cell counts and areas (Table VI). These data were similar to the proportion parameters, although the distinctiveness of Day 3 oxidant-formula bread was magnified, as reflected in the large-to-small cell area ratio measure.

We previously observed that oxidant-formula bread slices prepared on Day 3 had significantly thicker gas cell walls than did those prepared on other days. In light of these results, visual reexamination of digital images of oxidant-formula bread slices prepared on Day 3 showed that they had somewhat larger cells when compared with oxidant-formula bread prepared on other

TABLE VI
Relative Influence of Large Cells on the Total Number and Area of Detected Cells in Control and Oxidant-Formula Bread Baked on Different Days[a]

	Proportion of Total Cell Counts (%)	Proportion of Total Cell Areas (%)	Ratio of Large-to-Small Cell Counts	Ratio of Large-to-Small Cell Areas
Control				
Day 1	2.7 ± 0.4	58 ± 3	0.027 ± .005	1.40 ± 0.17
Day 2	2.9 ± 0.6	59 ± 5	0.030 ± .006	1.49 ± 0.32
Day 3	2.9 ± 0.2	59 ± 1	0.030 ± .003	1.44 ± 0.05
Mean[b]	2.84	58.8	0.029	1.44
Oxidized				
Day 1	2.1 ± 0.3	53 ± 2	0.021 ± .003	1.13 ± .10
Day 2	2.0 ± 0.2	52 ± 4	0.020 ± .002	1.09 ± .18
Day 3	2.2 ± 0.3	58 ± 4	0.023 ± .003	1.42 ± .27
Mean	2.08	54.3	0.021	1.21

[a] Large cells were defined a possessing cell areas greater than 4.0 mm^2 (2.26 mm equivalent diameter) (Fig. 4). Data based on cell detection method 2 (see Table IV).
[b] Mean parameter values, between control and oxidant formula bread, were significantly different ($P < 0.01$).

days. While the relationship between these atypical values for a few of the crumb grain features associated with oxidant-formula bread prepared on Day 3 is unclear, these results underscore the discriminatory power of the quantitative imaging system, which appears capable of readily exposing and measuring systematic differences in crumb grain structure (or departures from the norm) beyond the scope of visual inspection. Moreover, the two parameters listed in Table VI, related to the influence of large cells on the total area of detected cells, seem to provide measures of crumb grain uniformity consistent with subjective observations of greater uniformity, on average, for oxidant-formula bread than it does for the control, as would be expected. In quantitative terms, the crumb grain of oxidant-formula bread, as evaluated by the large-to-small cell area ratio feature, was 16% [(1.44 − 1.21)/1.44] more uniform than that of control loaves. In retrospect, it seems intuitively correct that the subjective perception of crumb grain uniformity might be related to the balance between large and small cells in terms of their perceived numbers or areas. As relatively large cells tend to dominate the visual scene, it is probably true, in general, that bread slices with relatively fewer cells above a given size threshold are perceived as being relatively more uniform.

CONCLUSIONS

A digital image analysis system has been developed for instrumental measurement of technologically relevant crumb grain features of baked bread, providing data that are directly interpretable. Computed parameters include crumb brightness, mean cell area, cell count density, mean CWT, and large-to-small cell area ratio as a derived measure of grain uniformity. The PC-based implementation represents a low-cost system that is precise, completely objective, and rapid. The time to process and generate quantitative data for a single bread slice was about 10 sec. Implementation of an adaptation of the *K*-means algorithm for image segmentation is a key feature of the system. This enables the computer to adapt or optimize image thresholding relative to variations in crumb brightness caused by variations in the breadmaking formula or processing conditions. In the absence of this or comparable optimization, inaccurate crumb grain measurements are generated.

While this article reports on the performance of the image analysis system applied to experimental bread produced under closely controlled laboratory conditions, the technology should be readily transferable to industry. One obvious application is the quantitative assessment of the effects of new or existing ingredients or processes on crumb grain. Another is quality control in the commercial production of white pan bread. Given the inherent capability of digital imaging to acquire and generate subtle information or details beyond the scope of human perception, it is very likely that even the most minor deviation from normal product specifications should be detectable, well in advance of it being noticeable by even the most experienced eye. Corrective measures could be taken sooner. The methodology should apply equally well to virtually any type of baked good product where internal appearance characteristics help to define product quality.

ACKNOWLEDGMENT

We wish to thank Yoshifumi Inoue for conducting the baking tests reported in this article. We also gratefully acknowledge the financial assistance from the Natural Sciences and Engineering Research Council of Canada and the United Grain Growers Ltd.

LITERATURE CITED

BAKER, J. C., and MIZE, M. D. 1941. The origin of the gas cell in bread dough. Cereal Chem. 18:19-34.

BERTRAND, D., LE GUERNEVÁ, C., MARION, D., DEVAUX, M. F., and ROBERT, P. 1992. Description of the textural appearance of bread crumb by video image analysis. Cereal Chem. 69:257-261.

BURHANS, M. E., and CLAPP, J. 1942. A microscopic study of bread and dough. Cereal Chem. 19:196-216.

HANDLEMAN, A. R., CONN, J. F., and LYONS, J. W. 1961. Bubble mechanics in thick foams and their effects on cake quality. Cereal Chem. 38:294-305.

HARALICK, R. M., and SHAPIRO, L. G. 1985. Survey image segmentation techniques. Comput. Vision Graphics Image Process. 29:100-132.

HARTIGAN, J. A. 1975. Clustering Algorithms. John Wiley and Sons: New York.

HEYNE, L., UNKLESBAY, K., and KELLER, J. 1985. Computerized image analysis and protein quality of simulated pizza crusts. 1985. Can. Inst. Food Sci. Technol. J. 18:168-173.

KAMMAN, P. W. 1970. Factors affecting the grain and texture of white bread. Baker's Dig. 44(2):34-38.

KILBORN, R. H., and IRVINE, G. N. 1963. A laboratory moulder for test baking. Cereal Sci. Today 8:341.

KILBORN, R. H., and TIPPLES, K. H. 1981a. Canadian test baking procedures. I. GRL remix method and variations. Cereal Foods World 26:624-628.

KILBORN, R. H., and TIPPLES, K. H. 1981b. Canadian test baking procedures. II. GRL-Chorleywood method. Cereal Foods World 26:628-630.

MOHS, K. 1924. The size of the pores in baked bread. Cereal Chem. 1:149-151.

PREWITT, J. and MENDELSOHN, M. 1966. The analysis of cell images. Ann. N. Y. Acad. Sci. 128:1035-1966.

PYLER, E. J. 1988. Baking Science and Technology. Sosland Publishing Co.: Merriam, KS.

SAHOO, P. K., SOLTANI, S., and WONG, A. K. C. 1988. A survey of thresholding techniques. Comput. Vision Graphics Image Process. 41:233-260.

SAPIRSTEIN, H. D. 1993. Digital image analysis and its applications in cereal science and industry. Pages 12-20 in: Proceedings of the 43rd Australian Cereal Chemistry Conference. C. W. Wrigley, ed. Royal Australian Chemical Institute: Melbourne.

SAPIRSTEIN, H. D., NEUMAN, M., WRIGHT, E. H., SHWEDYK, E., and BUSHUK, W. 1987. An instrumental system for cereal grain classification using digital image analysis. J. Cereal Sci. 6:3-14.

SMOLARZ, A., VAN HECKE, E., and BOUVIER, J. M. 1989. Computerized image analysis and texture of extruded biscuits. J. Texture Stud. 20:223-234.

SWALLOW, W. H., and BARUCH, D. W. 1986. Loaf evaluation. DSIR ISSN No. 0113-0129. Wheat Research Unit: Christchurch, NZ.

ZAYAS, I. Y. 1993. Digital image texture analysis for bread crumb grain evaluation. Cereal Foods World 38:760-766.

[Received September 10, 1993. Accepted April 6, 1994.]